TISSUE ENGINEERING: Part A
Volume 15, Number 10, 2009

DOI: 10.1089/ten.tea.2008.0670

Original Article

Preadipocytes Stimulate Ductal Morphogenesis and Functional Differentiation of Human Mammary Epithelial Cells on 3D Silk Scaffolds

Xiuli Wang, Ph.D.,[1] Xiaohui Zhang, Ph.D.,[1] Lin Sun, M.S.,[1] Balajikarthick Subramanian, M.S.,[1] Maricel V. Maffini, Ph.D.,[2] Ana Soto, M.D.,[2] Carlos Sonnenschein, M.D.,[2] and David L. Kaplan, Ph.D.[1,2]

Epithelial–mesenchymal interactions play an important role in regulating normal tissue development as well as tumor development for the mammary gland, but much is yet to uncover to reach a full understanding of their complexity. To address this issue, the establishment of relevant, surrogate, three-dimensional (3D) human tissue culture models is essential. In the present study, a novel 3D coculture system was developed to study the interactions between human mammary epithelial cells (MCF10A) and adipocytes, a prominent stromal cell type in native breast tissue. The MCF10A cells were cultured within a mixture of Matrigel™ and collagen in 3D porous silk scaffolds with or without predifferentiated human adipose–derived stem cells (hASCs). The presence of hASCs inhibited MCF10A cell proliferation, induced both alveolar and ductal morphogenesis, and enhanced their functional differentiation as evidenced by histology and functional analysis. The alveolar structures formed by cocultures exhibited proper, immature polarity when compared with native breast tissue. In contrast, only alveolar structures with reverted polarity were observed in the MCF10A monocultures. The effect of ductal morphogenesis in cocultures may correlate to hepatocyte growth factor secreted by the predifferentiated hASCs, based on results from a cytokine blocking assay. Taken together, this *in vitro* coculture model on silk scaffolds effectively reconstitutes a physiologically relevant 3D microenvironment for epithelial cells and stromal cells and provides a useful system to study tissue organization and epithelial morphogenesis in normal or diseased breast development.

Introduction

The mammary gland is one of several organs that change their architectural properties and functions during the different stages of the reproductive cycle (puberty, pregnancy, menopause, and senescence) via reciprocal interactions between epithelial cells and the stromal tissue under the cyclical and tonic effects of steroid and polypeptide hormones. *In vivo* recombination studies have elegantly demonstrated that mammary stromal cells not only direct, but also redirect the developmental fate of normal and tumorigenic mammary epithelial cells.[1–3] However, due to the complex *in vivo* environment, detailed mechanistic studies are difficult to interpret in those animal models.

A number of cell lines in two-dimensional (2D) conditions have been often used to better understand cellular-based phenomena like differentiation and even carcinogenesis under the somatic mutation theory's perspective. However, these stationary 2D cell cultures recapitulate neither the differentiated structures nor the functions of the mammary epithelium *in vivo*, and are inadequate for assessing the role of stroma in the development and carcinogenesis of breast tissue. An enormous potential exists in the use of three-dimensional (3D) tissue culture models as surrogates for breast tissues. During the past two decades, investigators have converged to establish simple yet effective 3D models of the mammary tissue by using collagen gels or reconstituted basement membrane from mouse,[4–6] and many key molecular, structural, and mechanical cues important for maintaining the architecture and function of breast tissue *in vitro* have been identified. However, few studies of *in vitro* 3D tissue systems have focused on the interactions between human adipocytes and human epithelial cells, despite of the fact that adipocytes are one of the predominant constituents of the resting mammary gland and that the first stages of carcinogenesis take place in an adipocyte-rich environment.[7]

Several studies aimed at defining differentiation patterns in mammary development used a rodent nonmammary cell line, 3T3-L1 preadipocytes, primary mammary preadipocytes,

[1]Departments of Biomedical and Chemical and Biological Engineering, Tufts University, Medford, Massachusetts.
[2]Department of Anatomy and Cellular Biology, Tufts University School of Medicine, Boston, Massachusetts.

or excised mouse mammary gland fat pads.[7–9] However, it is still unknown whether or not distinct signal pathways exist between human and rodent mammary development and oncogenesis.

Coculture of human mammary epithelial cells and adipocytes from the same patient in a collagen matrix was first reported by Huss and Kratz,[10] and these authors only characterized the growth profile of the cocultures, while no detailed morphology and function of the system was described. A better understanding of the complex interactions between epithelial cells and adipocytes would benefit from a well-characterized, relevant 3D coculture model of human breast tissue.

Although hydrogel culture systems, such as collagen and/or Matrigel, have been utilized to construct *in vitro* 3D culture models of breast tissue,[4–6,11,12] spontaneous contraction, limited mass transport, and rapid degradation after cellular transfer/implantation suggest that data collected with these culture systems be considered with caution. Our previous studies have demonstrated that silk proteins, as naturally occurring degradable fibrous proteins with unique mechanical properties, exhibit excellent biocompatibility and controlled slow degradation. These features offer major benefits in the establishment of long-term 3D cultures as well as for *in vivo* transplantation for regenerative medicine goals.[13–16] In the present study, the nontumorigenic, human breast epithelial MCF10A cells were cocultured with one of the prominent mammary stromal cells, that is, (pre)adipocytes, within 3D porous silk scaffolds. We hypothesized that breast epithelial cells growing in a 3D microenvironment provided by the preadipocytes and silk scaffolds would generate mammary tissue–like structures that would more closely resemble the *in vivo* mammary morphology and function. The 3D coculture model was characterized by morphology and function, and a mechanism related to ductal morphogenesis was explored.

Materials and Methods

Cell and tissue culture materials

Dulbecco's modified Eagle's medium (DMEM)/F12, fetal bovine serum (FBS), horse serum, penicillin–streptomycin (P/S) solution, human epidermal growth factor (hEGF), human hepatocyte growth factor (hHGF), human insulin, trypsin–EDTA, and Trizol were purchased from Invitrogen (Carlsbad, CA). Hydrocortisone, cholera toxin, biotin, D-pantothenate acid, dexamethasone, isobutylmethylxanthine (IBMX), and thiazolidinedione (TDZ) were from Sigma-Aldrich (St. Louis, MO). Growth factor–reduced Matrigel™ and rat tail type I collagen were from BD Biosciences (San Jose, CA). Anti-hHGF R (c-met) antibody was from R&D Systems (Minneapolis, MN). All other substances were of analytical or pharmaceutical grade and obtained from Sigma-Aldrich. Silkworm cocoons were kindly supplied by M. Tsukada (Institute of Sericulture, Tsukuba, Japan) and Marion Goldsmith (University of Rhode Island, Cranston, RI).

Preparation of aqueous-derived silk fibroin scaffolds

Three-dimensional aqueous-derived silk fibroin scaffolds were prepared according to the procedures described in our previous studies.[15,17] Briefly, a 6.5% (w/v) silk fibroin solution was prepared from *Bombyx mori* silkworm cocoons. The cocoons were extracted in a 0.02M Na_2CO_3 solution, dissolved in a 9.3 M LiBr solution, and subsequently dialyzed against distilled water. To form the scaffolds, 4 g of granular NaCl particles was added to 2 mL of a silk fibroin solution in Teflon cylinder containers and allowed to sit at room temperature for 1–2 days. Then, the containers were immersed in water to extract the salt from the porous scaffolds for 2 days. The pore size of the resultant scaffolds was 500–650 μm, as evaluated by scanning electron microscopy (Zeisss ULTRA 55, Solms, Germany, Fig. 1). The scaffolds were cut into discs (5 mm diameter × 2.5 mm thickness), dried in a fume hood, and autoclaved for further sterile cell cultivation experiments. Before cell seeding, the scaffolds were conditioned with the coculture medium overnight.

Cell maintenance and differentiation

MCF10A cells (American Type Culture Collection, Manassas, VA) were cultivated in DMEM/F12 supplemented with 0.1 μg/mL cholera toxin, 10 μg/mL insulin, 0.5 μg/mL hydrocortisone, 20 ng/mL human epidermal growth factor, 5% horse serum, and 1% P/S solution. Human adipose–derived stem cells (hASCs) were isolated according to previously published methods from subcutaneous adipose tissue donated with written consent by healthy volunteers (women; mean age, 47 years) undergoing elective liposurgery.[18] The work was reviewed and approved by the Pennington Biomedical Research Center Institutional Review Board. hASCs were maintained in DMEM/F12 containing 1.0 g/L glucose and 10% FBS, and allowed to achieve confluence before they were induced to differentiate (designated as day 0). An adipocyte differentiation medium (medium I) composed of 3% FBS, 1% P/S, 500 μM IBMX, 1 μM dexamethasone, 17 μM D-pantothenate acid, 33 mM Biotin, 5 μM TZD, and 1 μM insulin in DMEM/F12 medium was applied to induce hASC differentiation (designated as day 1–7). After 1 week (i.e., on day 8), the medium was replaced with adipocyte maintenance media (medium II), which is similar to the differentiation medium I except for the absence of IBMX and thiazolidinedione. Cells were then fed every other day with medium II until they were used for either histology characterization or

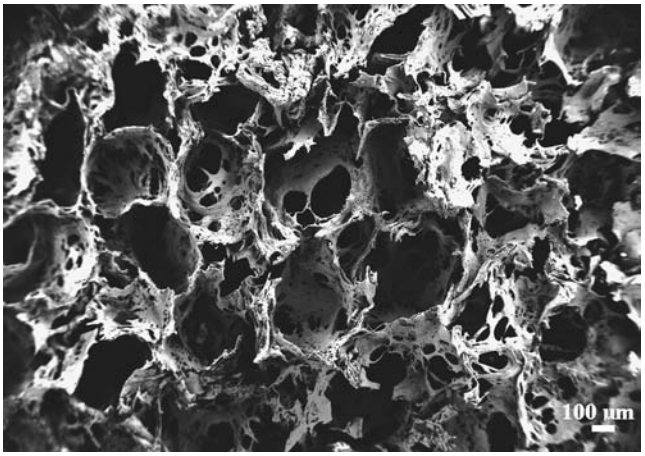

FIG. 1. Scanning electron microscopy image of porous silk scaffolds (pore size, 500–650 μm).

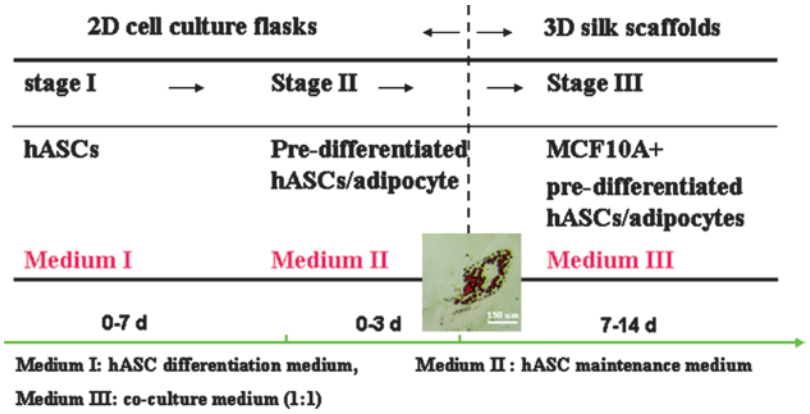

FIG. 2. A three-step experimental design for the coculture on silk scaffolds. Stage I, inducing hASCs cells differentiation into predifferentiated hASCs with the differentiation medium I in cell culture flasks; Stage II, maintaining the phenotype of predifferentiated hASCs with the maintenance medium II in cell culture flasks, image showing the cytoplasmic triglyceride droplets in the differentiated hASCs (oil red-O staining); Stage III, coculturing MCF10A cells and predifferentiated hASCs with the medium III on three-dimensional silk scaffolds. hASCs, human adipose–derived stem cells. Color images available online at www.liebertonline.com/ten.

coculture experiments. By day 3, the elongated fibroblast-like hASCs became round; by day 8, small cytoplasmic triglyceride droplets were evident (Fig. 2). For coculture experiments, a combined medium (MCF10A medium:hASC medium II = 1:1) was used. The coculture medium was previously tested to assure proper growth and behavior of each type of cells. All cells were incubated at 37°C and 5% CO_2.

Preparation of the 3D cocultures on silk scaffolds

Rat tail type I collagen was used according to the manufacturer's instructions. The mixed Matrigel–collagen gel was prepared using a 1:1 ratio of GFR Matrigel and type I collagen solution keeping the final collagen concentration at 1.0 mg/mL. In coculture, MCF10A and predifferentiated hASCs (on day 9–10) were mixed with the Matrigel–collagen solution and seeded on the preconditioned silk scaffolds in a 2:1 ratio keeping the number of epithelial cells constant (60,000 cells/scaffold). After gelation at 37°C, in a 5% CO_2 atmosphere for 2 h, the cell-loaded scaffolds were transferred into nontreated 12-well plates; coculture medium was added gently to avoid disturbing the scaffolds. Monocultures of MCF-10A cells in the same conditions with the same seeding density served as control. All cultures were incubated at 37°C and 5% CO_2 in a 100% humidified incubator for 2 weeks, and the medium was changed every 2 days.

In some experiments, to determine the different types of cells in the cocultures, MCF10A cells and predifferentiated hASCs were labeled with CellTracker™ DiI and CellTracker™ Green CMFDA separately following the protocols provided by the manufacturer (both from Invitrogen). Briefly, adherent cells at desired confluence in T75 cm^2 culture flasks were incubated with the prewarmed 25 μM CellTracker for 30–40 min under growth conditions. Then, the dye was replaced with fresh, prewarmed medium, and the cells were incubated for another 30 min at 37°C. After washing with DPBS two times, the labeled cells were harvested for seeding. Morphologic development was observed by either phase contrast microscopy (Zeisss Axiovert S100) or confocal laser scanning microscopy (CLSM; Leica SP2, Oberkochen, Germany).

Cell viability in 3D scaffolds

To assess cell viability by calcein-AM/EthD-1 staining (Invitrogen), cell-containing scaffolds were cut into four pieces and incubated with the diluted dye solution at 37°C for 30–45 min as described before.[19] After washing with PBS, preparations were observed under CLSM. Only live cells with intracellular esterase activity can digest nonfluorescent calcein-AM into fluorescent calcein (green). Dead or dying cells containing damaged membranes allowed the entrance of EthD-1 to stain the nuclei (red).

Cell proliferation on 3D scaffolds

Cell proliferation on 3D silk scaffold was determined by DNA content analysis. Briefly, scaffolds were chopped into pieces in 1 mL 0.2% Triton X-100 and 5 mM $MgCl_2$ solution. DNA content was measured using PicoGreen™ DNA Assay according to the protocols of the manufacturer (Molecular Probes, Eugene, OR). Samples ($n = 3$ per group in the same experiment, three repeats) were measured through a fluorometer at an excitation wavelength of 480 nm and an emission wavelength of 530 nm.

Histology and immunofluorescence staining

Constructs were harvested and fixed in 4% formaldehyde for histological and immunofluorescence staining at time points indicated earlier. Hematoxylin and eosin staining was conducted as described previously.[19] For immunofluorescence staining, deparaffinized sections (5 μm) were heated by microwave treatment (~95°C) in an antigen-retrieval solution (Fisher, Pittsburgh, PA) for 15 min. After sequential treatment of penetration and blocking, sections were incubated with primary antibodies from mouse as follows: anti-human Ki67 (1:80; BD Biosciences), anti-human Col-IV (1:50; Invitrogen), anti-human GM130 (1:80; BD Biosciences), anti-human sialomucin (1:20; Abcam, Cambridge, MA), anti-human casein (1:20; Abcam), and anti-human E-cadherin (1:40; Abcam). Adjacent sections served as negative controls, which were processed with the same procedures except incubation with PBS buffer instead of the primary antibodies. FITC or TRITC-conjugated goat anti-mouse IgG (1:100; Sigma, St. Louis, MO) were used as secondary antibodies. For immunohistochemical staining of Ki67, a mouse ABC staining kit from Santa Cruz Biotechnology (Santa Cruz, CA) was used following the manufacturer's protocol, and the number of positive staining cells in different microscopic fields (at least 10 microscopic fields per slide, three slides per group-redifferentiatee) was counted under an upright microscope (Olympus BH-2, Tokyo, Japan). Human normal breast tissue sections (provided by Tufts Medical Center, Boston, MA) served as positive controls. Either propidium iodide

(5 μg/mL; Invitrogen) or DAPI (2 μg/mL; Research Organics, Cleveland, OH) was used to counterstain the cell nucleus. Images were captured with Leica SP_2 CLSM.

Real-time RT-PCR analysis

To prepare samples for RT-PCR analysis, scaffolds loaded with MCF10A (labeled by DiI CellTracker) and predifferentiated hASCs (labeled by CMFDA CellTracker) were cut into smaller pieces and multitrypsinized with 0.25% trypsin–EDTA at 37°C. After harvesting all the cells from the scaffolds, fluorescence-activated cell sorting was used to sort the different cell types. Total RNA was extracted from cells using an RNAeasy Mini Kit (Qiagen, Valencia, CA) following the supplier's instructions. Total RNA concentration was determined by OD_{260}. After synthesis of cDNA using a high-capacity cDNA archive kit (ABI Biosystems, Foster City, CA), real-time PCR was conducted and monitored with an ABI Prism 7000 Sequence Detection System. TaqMan Gene Expression assay kit (Applied Biosystems, Foster City, CA) was used for transcript levels of α-casein (Hs00157136_m1) and hHGF (Hs00300159_m1) following the vendor's protocol. The final data were analyzed by ABI Prism 7000 Sequence Detection Systems version 1.0 software supplied by the vendor. The Ct value for each sample was defined as the cycle number at which the fluorescence intensity reached a certain threshold where amplification of each target gene was within the linear region of the reaction amplification curves. The relative expression level for each target gene was normalized by the Ct value of TaqMan human housekeeping gene *GAPDH* (Hs99999905_m1) using an identical procedure (2ΔCt formula; Perkin Elmer User Bulletin #2). Each sample was analyzed in triplicate.

hHGF inhibition

To neutralize hHGF activity, MCF10A cells were incubated overnight in growth medium supplemented with 8 μg/mL anti-hHGF R (*c-Met*) antibody. Then, the pretreated MCF10A cells were mixed with predifferentiated hASCs and seeded either in eight-well chamber slides or on silk scaffolds as described above. The eight-well chamber slide was used to facilitate morphological observation under phase contrast microscopy. Coculture media were supplemented with anti-hHGF R antibody at the indicated concentration. The inhibition targeted an epithelial cell receptor for hepatocyte growth factor (HGF) to prevent disruption of potential autocrine interactions between HGF and hASCs, and to account for the presence of serum-derived trace amounts of HGF in the culture medium. The working concentration of the receptor blocking antibody was selected based on the results of preliminary dose response experiments.

Statistical analysis

All reported values were averaged ($n = 3$ repeats except for the specific explanation) and expressed as mean ± standard deviation. Statistical differences were determined by Student's two-tailed *t*-test, and differences were considered statistically significant at $p < 0.05$.

Results

Proliferation of epithelial cells and/or predifferentiated hASCs on 3D silk scaffolds

As a first step in defining coculture effects on epithelial cells, a coculture medium was tested in which the ratio between MCF10A maintenance medium and predifferentiated hASC medium II was 1:1. The results showed that on 3D silk scaffolds, the cell numbers in the monoculture group (MCF10A cells) or in coculture group (MCF10A and hASC) increased gradually during 9-day culture in the defined coculture medium (Fig. 3A). In our preliminary studies, no significant difference was observed between the native medium and the coculture medium when the cells were assayed for growth curves in 2D culture systems (data not shown). Thus, we concluded that the coculture medium was capable of supporting the growth of both types of cells.

To determine the effect of predifferentiated hASCs on the proliferation of MCF10A cells, Ki67 expression, an important cellular marker for proliferation, was detected by immunohistochemical staining. After a 1-week culture in the silk scaffolds, the number of $Ki67^+$ MCF10A cells was lower in the cocultures with predifferentiated hASCs than in the monoculture of MCF10A cells ($p < 0.05$) (Fig. 3B), which indicates that the hASCs present in the coculture system may

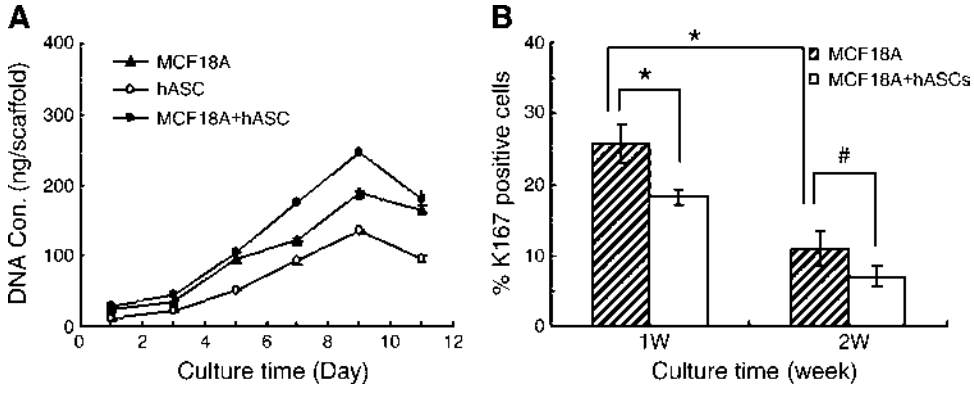

FIG. 3. (**A**) DNA quantification by PicoGreen DNA content assay showed cells proliferation in the monoculture or cocultures models on three-dimensional silk scaffolds. (**B**) Inhibition effect of predifferentiated hASCs on MCF10A cell proliferation assayed by semi-quantitive analysis of Ki67 staining. Only positive staining cells within epithelial structures were counted in different microscopic fields ($n = 10$ per slide, 3 slides per group). A significant decrease of the $Ki67^+$ MCF10A cells was observed in the cocultures during the first week, and the percentage of positive staining cells deceased over time ($^*p < 0.05$, $^\#p > 0.05$).

inhibit proliferation of the MCF10A cells. However, the percentage of $Ki67^+$ cells decreased over time in both of the groups. After a 2-week culture, no significant difference was observed between these two groups. This might be partly explained by the lower proliferation rate of MCF10As once they become more differentiated during culture.

Growth profiles of epithelia cells on 3D silk scaffolds

After 24 h, MCF10A cells and predifferentated hASCs were evenly distributed throughout the silk scaffolds mostly as single cells or small aggregates of two to three cells. Epithelial structure began to organize after 3 days in coculture; by the sixth day, some acinar and duct-like structures were formed by the MCF10A cells in the cocultures. These structures could be identified based on the use of CellTracker staining (Fig. 4A). The size of acinar and duct-like structures in the cocultures increased with time, especially from day 4 to 10. Due to poor transparency of the scaffolds, no structures could be observed by phase contrast microscopy after 2 weeks in culture. This loss in resolution was likely due to the higher cell numbers and the enriched extracellular matrices (ECMs) formed during this time frame. In contrast to the coculture group, only acinar structures were observed in the monocultures of MCF10A cells, even beyond the 2-week culture time (Fig. 4B).

The viability of the cells in the silk scaffolds was also evaluated by live/dead staining. After 1 week in culture, the majority of the cells in both groups (coculture and monoculture) exhibited good viability (Fig. 4C, D), suggesting that both the silk scaffold and the culture matrix provided a suitable microenvironment for the growth of MCF10As and hASCs.

Morphological characteristics of the epithelial structures formed on 3D silk scaffolds

Hematoxylin and eosin staining revealed detailed growth profiles of MCF10A cells either in monocultures or in cocultures with predifferentiated hASCs. Consistent with our observation under phase contrast microscopy, MCF10A cells in cocultures formed both acinar and duct-like structures in the mixed Matrigel–collagen matrix in contrast to the exclusive formation of acinar structures in the monocultures. After culture for 2 weeks, the size of acinar structures increased significantly. In addition, as early as 1 week of culture, a lumen was observed in the center of the acini and their nuclei were located to the basal side, an indicator of cell polarity (Fig. 4E, F).

To further characterize the epithelial structures formed on 3D silk scaffolds, expression of E-cadherin and collagen IV was detected by immunofluorescent staining. E-cadherin, a marker for epithelial cell junctions, was observed in both acinar and duct-like structures (Fig. 5A). Collagen IV, a major component of the basement membrane, was also found at the basal side of the acinar structures, providing further evidence for the tissue-like integrity of the epithelial structures formed on 3D silk scaffolds (Fig. 5B).

GM130, a large coiled-coil protein of *cis*-Golgi apparatus (GA) and sialomucin (CD164), a transmembrane molecule encoded by the *MUC1* gene, are physiologically expressed at the apical side of mammary acini *in vivo*, and are two important markers for mammary functional polarity. As shown in Figure 6, expression of these two proteins was observed in the acinar structures formed within the cocultures with predifferentiated hASCs. Their expression was enriched on the apical and lateral sides of the MCF10A cells, while no staining was observed on the basal side. Compared with breast tissue *in vivo*, however, this expression pattern of GM130 and CD164 was far less focused on the apical side, which may indicate the immaturity of the acinar structures formed on the silk scaffolds during this relatively short time frame of culture. Interestingly, a reverse polarity was observed in the monoculture group where these two markers adopted basal location instead of either apical or lateral location.

Functional differentiation of the epithelial structures formed on 3D silk scaffolds

Casein expression is an indicator of the functional differentiation of epithelial cells. To determine whether the presence of predifferentiated hASCs enhanced function as well as morphological differentiation of epithelial cells on silk scaffolds, α-casein gene expression in MCF10A cells was analyzed by real-time RT-PCR. Compared with the monocultures, α-casein mRNA level was significantly up-regulated in the cocultured MCF10A cells. Additionally, expression increased with time; after 2 weeks in culture, transcript level was significantly higher than that at 1 week. This result indicates that MCF10A cells cocultured with predifferentiated hASCs became more functional with prolonged culture time (Fig. 7A). With immunofluorescent staining, higher casein expression was observed in the coculture group in comparison with the monoculture group (Fig. 5C_1, C_2). These data provide further evidence that predifferentiated hASCs present in coculture may contribute to MCF10A cell functional differentiation on 3D silk scaffolds.

HGF secreted by hASCs mediates ductal morphogenesis of epithelial cells

A previous study by Soriano *et al.*[20] demonstrated that HGF secretion by stromal cells may act as a mediator in inducing mammary gland development. Consistently, we observed *HGF* gene expression in the cocultured hASCs as measured by RT-PCR. The expression level decreased over time (1-week vs. 2-week), which may be explained by the differentiation of the hASCs during the coculture, since undifferentiated preadipocytes have been reported to exhibit a higher capability for HGF secretion in comparison with terminal differentiated adipocytes *in vitro*.[21]

To determine whether HGF might be one of the cytokines secreted by hASCs that stimulates ductal morphogenesis by epithelial cells, the MCF10A cells were preincubated with anti-rhHGF R (*c-Met*) antibody. Different concentrations of anti-rhHGF R (2–8 μg/mL) were added to the coculture maintenance medium as described earlier. This resulted in a dose-dependent inhibition of duct-like structure formation (Fig. 8). The number of ductal-like structures decreased significantly after anti-rhHGF R addition (day 6). However, ductal morphogenesis was not completely inhibited even at the highest concentration of anti-rhHGF R (8 μg/mL).

Discussion

In the studies reported herein, a physiologically relevant 3D coculture model was developed for the study of normal

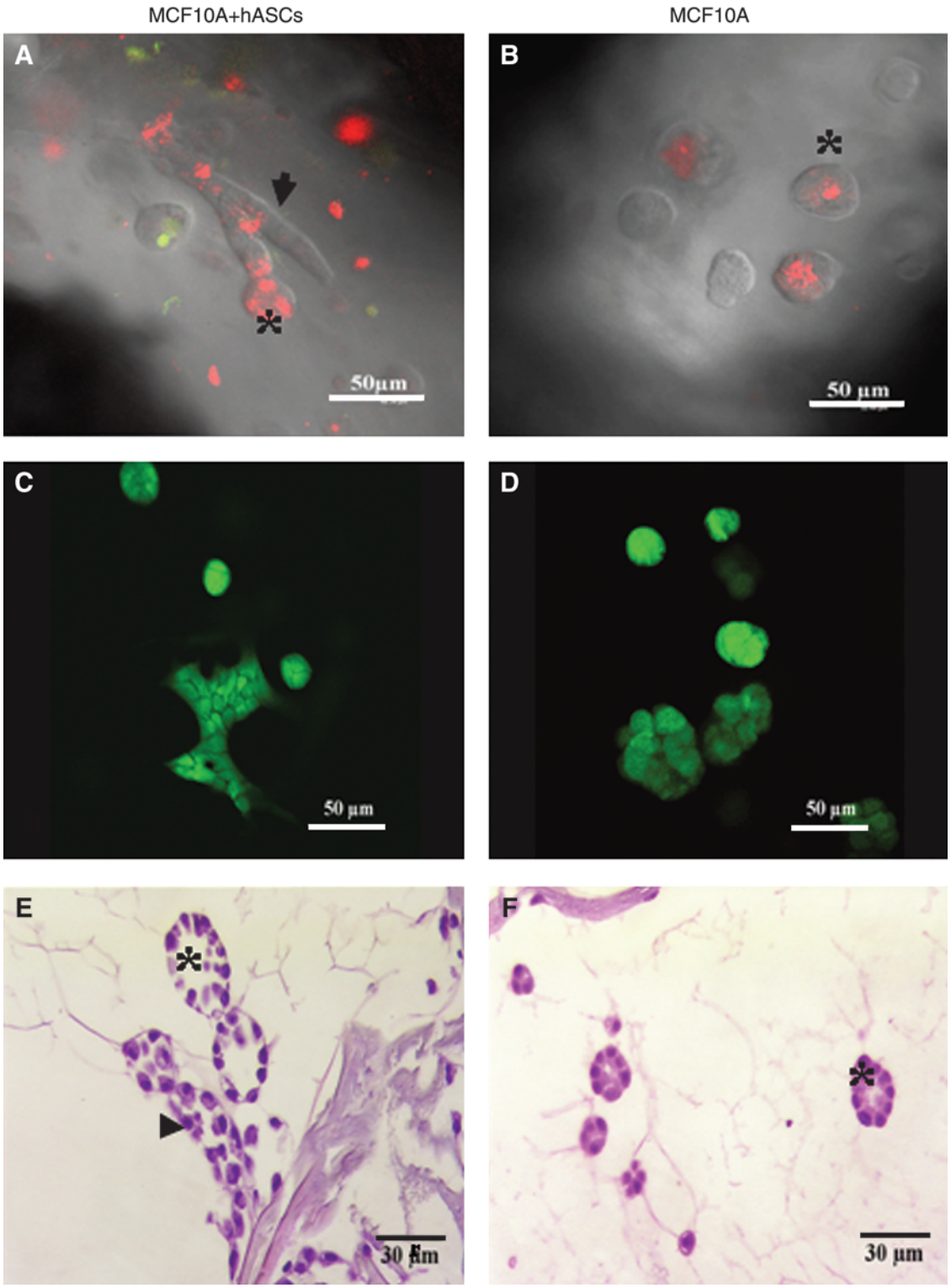

FIG. 4. Growth profile and viability of MCF10A cells in the monoculture or coculture constructed on silk scaffold (at day 6). Confocal images showed both alveolar and ductal-like structures formed in cocultures (**A**), while only alveolar structures were observed in the monocultures (**B**) (red, MCF10A cells labeled with DiI; green, hASCs labeled with CMFDA). An ideal viability of MCF10A cells in different groups detected by Live/Dead staining (**C, D**). Hematoxylin and eosin staining showed detailed morphological characteristics of the epithelial structures formed by MCF10A cells in different culture groups (**E, F**). Clearer lumen structures were observed in the cocultures (**F**). Arrowhead denotes ductal-like structure; asterisk denotes alveolar structure. Color images available online at www.liebertonline.com/ten.

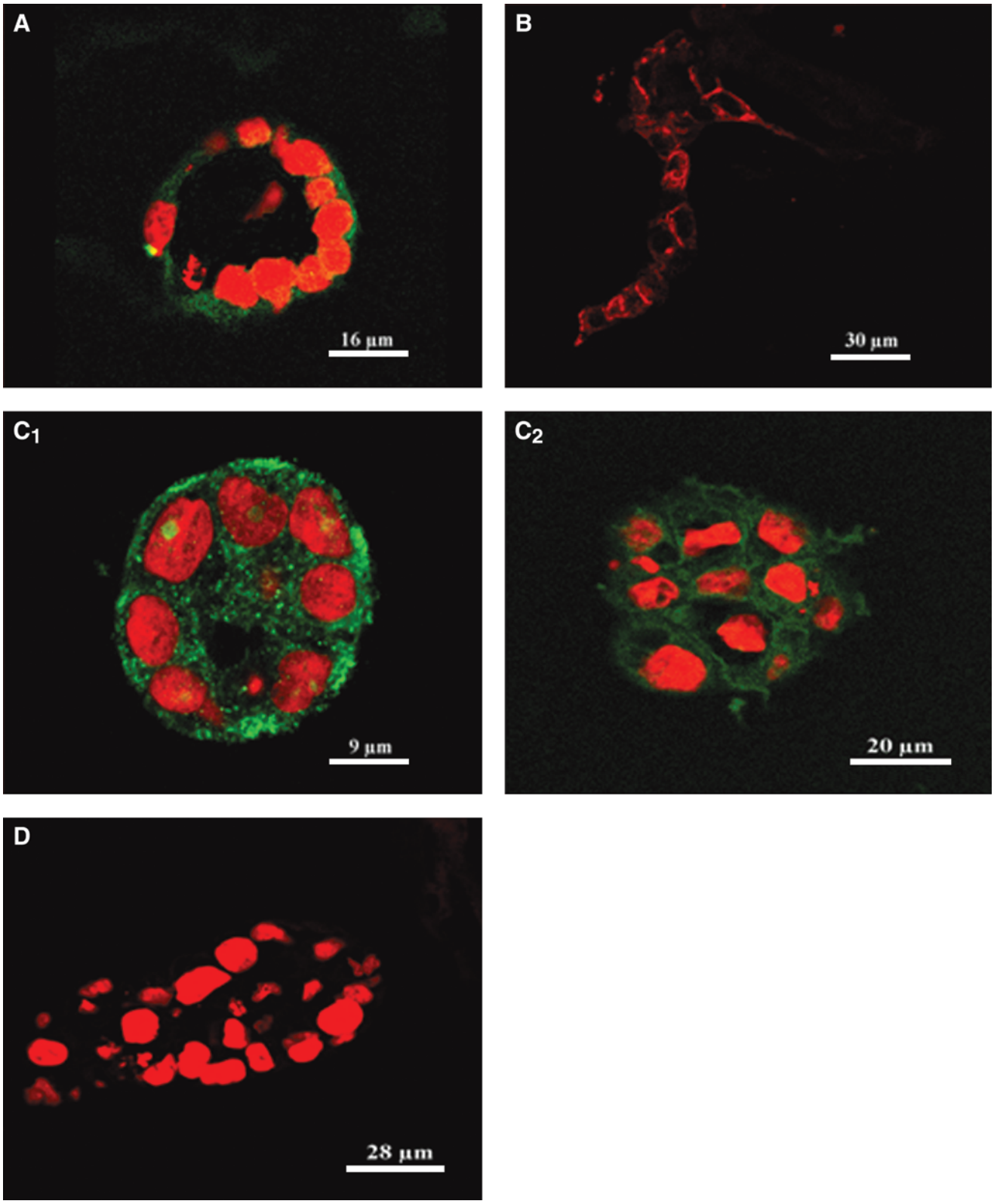

FIG. 5. Immunostaining images showed the morphological characteristics of the epithelial structures formed by cocultured MCF10A cells on silk scaffold. (**A**) Collagen staining showed the basement membrane formation of the alveolar structure. (**B**) Positive E-cadherin staining indicated the integrity of the tissue-like structures. (**C**) Higher casein expression level was observed in cocultures (**C1**) than in the monocultures (**C2**). (**D**) Antibody replaced by PBS served as negative control, and cell nuclei were counterstained by propidium iodide. Color images available online at www.liebertonline.com/ten.

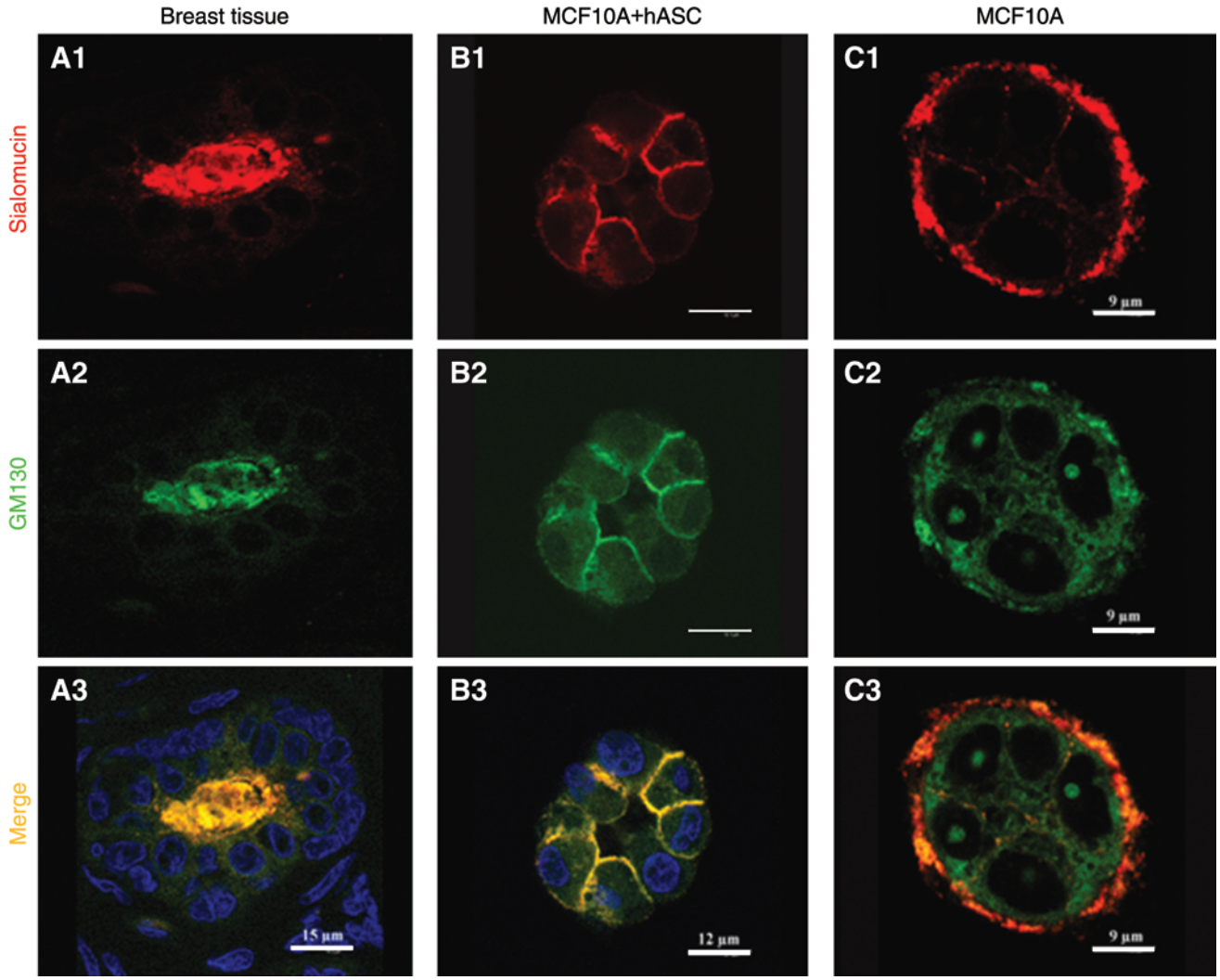

FIG. 6. Immunostaining images of sialomucin (red) and GM130 (green) showed the correct polarity of the alveolar structures formed by cocultured MCF10A cells in silk scaffold (**B1–B3**, day 6). Cell nuclei were counterstained by DAPI (blue), while reversed polarity was observed in the monoculture (**C1–C3**, day 6). Human breast tissue served as positive control (**A1–A3**). Color images available online at www.liebertonline.com/ten.

and altered human breast development *in vitro*. This 3D coculture model system offers several significant advantages over previously described experimental models because of the partial reconstitution of the 3D microenvironment of normal mammary gland *in vivo*. First, both epithelial cells and hASCs are from human sources, to provide reasonable assurance that the information provided by this 3D culture model is applicable to human breast development. Second, the use of the immortalized cell line MCF10A, rather than normal primary breast tissue, eliminates heterogeneity associated with different donors at different developmental or disease states. In addition, the procedures employed in this study preclude the need to isolate and purify epithelial cells from breast tissue. Third, it has been well known that the main ECM component of human mammary gland is type I collagen, while several glycosaminoglycans and basement membrane components such as collagen type IV and laminins are also present.[12] Therefore, to more closely mimic the microenvironment *in vivo*, a defined, mixed matrix composed of collagen I and GFR Matrigel was adopted in this 3D coculture model. Finally, porous silk scaffolds were involved in the coculture model, which not only provides architectural and physical support for the cocultures, but also offers future possibilities for implanting or explanting these constructed 3D models *in vivo* with the aims of cell replacement therapy and/or cell–microenvironment interaction study *in vivo*. Most importantly, the controlled degradation of silk allows tissue-like structures to form *in vivo*, without the premature loss of transport through the matrices that would lead to necrotic zones, a common issue with most other degradable polymeric scaffolds.

To characterize the 3D coculture model *in vitro*, we first evaluated the influence of predifferentiated hASCs on the growth of MCF10A cells. Efforts in this direction have met with somewhat conflicting results mainly due to the different methodology used.[6,22,23] However, a consensus indicate that while cocultured stromal cells affect the growth of epithelial cells, this effect was dependent on the type of stromal cells,

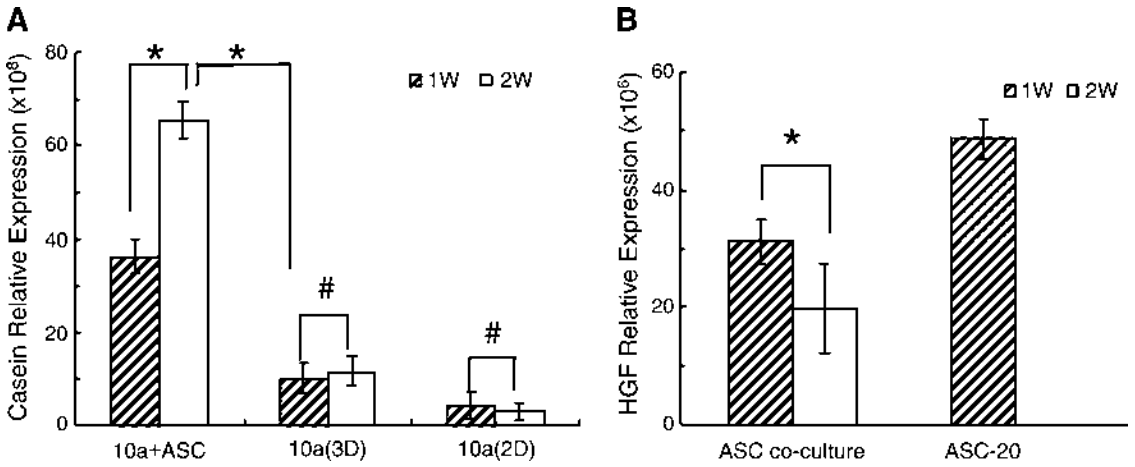

FIG. 7. Transcript levels of (α-casein (MCF10A cells, **A**) and hepatocyte growth factor (hASCs cells, **B**) by real-time RT-PCR at the indicated time points. Significantly increased expression of casein-α was observed in MCF10A cells cocultured with predifferentiated hASCs ($n = 3$, $^{*}p < 0.05$, $^{\#}p > 0.05$).

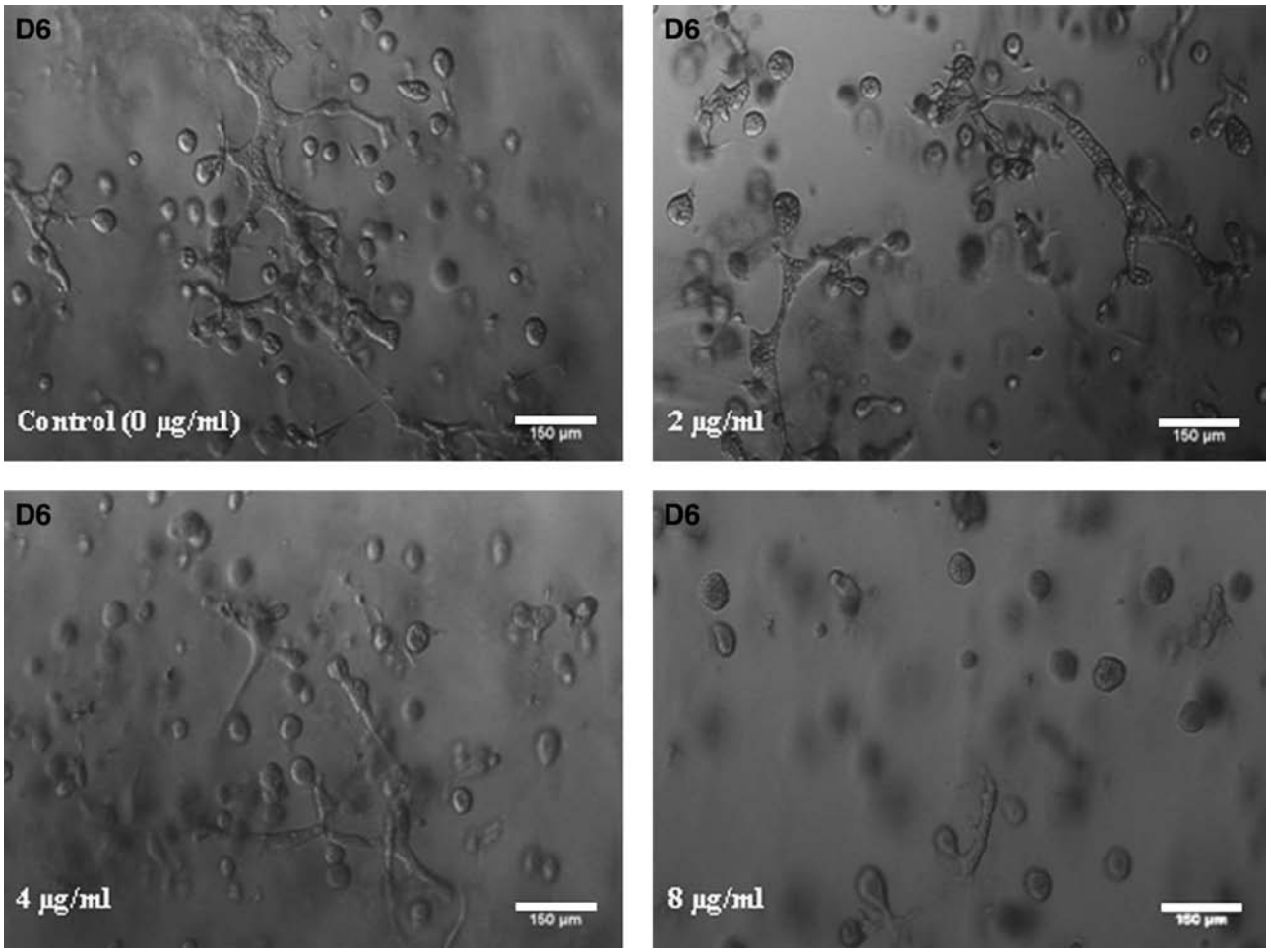

FIG. 8. Growth profile of MCF10A cells cocultured with predifferentiated hASCs in an eight-well chamber slide after different concentrations of anti-hHGF R (c-met) were supplemented into the coculture medium. A dose-dependent inhibition effect of anti-hHGF R (*c-Met*) on MCF10A cell ductal morphogenesis was observed as evidenced by the decreased number and shorter length of ductal-like structures in coculture. hHGF, human hepatocyte growth factor.

the characteristics of the epithelial cells, and the culture conditions utilized.[24] In the present study, an inhibitory effect of hASCs on the growth of MCF10A cells was observed in 3D coculture, with evidence of a lower percentage of Ki67 positive staining MCF10A cells in the cocultures when compared with monocultures. This result is consistent with the more differentiated phenotype exhibited by the MCF10A cells cocultured with predifferentiated hASCs, because in the development of breast tissue *in vivo*, once epithelial cells become more differentiated, their proliferation is arrested.[25]

Epithelial structures formed in the presence or absence of predifferentiated hASCs were further evaluated. Both acinar and duct-like structures were generated in the cocultures; however, only acinar structures were found when MCF10A cells were cultured alone. This indicates that direct and/or indirect cellular interactions occurred in the constructed 3D coculture system, and predifferentiated hASCs induced ductal morphogenesis effect on the epithelial cells.

With regard to ductal morphogenesis, a study by Soriano *et al.* revealed that HGF secreted by mouse fibroblasts stimulated extensive development of branching duct-like structures by cloned mouse mammary gland epithelial cells.[20] HGF is a pleiotropic cytokine that was originally identified in the serum of partially hepatectomized rats. HGF binds to a membrane-spanning tyrosine kinase receptor encoded by the c-met protooncogene, which is thought to be present in the plasma membranes of many tissues such as liver, mammary gland, kidney, and lung.[26,27]

hASCs also secrete a wide profile of cytokines, including HGF, proinflammatory, and haematopoietic cytokines.[21] Due to the indispensable role of HGF during mammary duct morphogenesis demonstrated by several previous studies[20,26,27] and our RT-PCR results of *hgf* gene transcript expression in the predifferentiated hASCs, we herein propose that HGF may act as a paracrine mediator of morphogenetic epithelial–mesenchymal interactions in the 3D coculture model. This hypothesis is supported by the result from hHGF blocking experiments with anti-hHGF R (*c-Met*), where few duct-like structures were observed after the blocking. However, when the monocultures were supplemented with different concentrations of exogenous hHGF (5–20 ng/mL) with the aim of replacing the predifferentiated hASCs in the 3D coculture model, no ductal morphogenesis occurred (data not shown). In addition, we also failed to recapitulate the process of ductal morphogenesis once predifferentiated hASCs and MCF-10A cells were physically separated by sequential inoculation on silk scaffolds (i.e., seeding mixture of Matrix-MCF10A cells in silk scaffolds with preseeded (pre)adipocytes). Thus, we conclude that both the paracrine factors (including HGF and other undetermined factors) and direct cellular contact might be required for ductal morphogenesis of MCF-10A cells in the coculture model. More extensive studies are still needed to further characterize the whole events.

Besides the effect of ductal morphogenesis, more differentiated and functional epithelial structures also were observed in the cocultures as evidenced by the expression patter of sialomucin and GM130 proteins as well as the enhanced casein expression level. Compared with the inside-out polarity in the monocultures, we hypothesize that predifferentiated hASCs might contribute to the appropriate polarity of MCF10A cells in 3D coculture, even though the polarity would be less mature in comparison with native breast tissue. Mammary glandular epithelial cells are polarized, have specialized cell–cell contacts, and are attached to an underlying basement membrane. The development and maintenance of this polarized structure is critical for functional integrity of the gland.[28] However, how polarity is generated and maintained is unclear. A number of studies suggest that laminin-1 and myoepithelial cells are important determinants of those processes. For example, Gudjonsson *et al.* demonstrated that inside-out polarity formed in collagen gel–embedded human primary mammary epithelial cells could be corrected by either laminin-1 addition or normal myoepithelial cell coculture.[29] In the present study, the inside-out polarity of the epithelial structures also was observed, which might be explained by (1) insufficient laminin-1 in the culture matrix composed by collagen type I and GFR Matrigel or (2) inability of laminin-1 synthesis by luminal epithelial cells in the monoculture. Coculture with predifferentiated hASC partly reverses the polarity, which indicates that stoma–epithelial interactions play important roles in promoting the formation of more differentiated and functional epithelial structures.

It should be noted that although the presence of predifferentiated hASCs in the coculture system consistently exerted similar effects on epithelial structure morphogenesis, the magnitude of the effects was confounded by the varied differentiated efficiency of hASCs. In keeping with the *in vivo* condition, a mixed population of preadipocytes and terminally differentiated adipocytes was used in present study, but it is difficult to specify their ratio. To minimize the variation in hASCs' behavior associated with donor source, long-term culture on tissue culture plastic, and induction effects,[30] only low passage number hASCs (passage 3–4) from the same donor were utilized for the specified days of predifferentiation (7 days).

It should be also pointed out that the time of culture is important for the interpretation of interactions between mammary epithelial cells, stromal cells, and matrix components. Thus, a long-term 3D coculture model of human breast tissue would be valuable in determining the molecular mechanisms of normal development or carcinogenesis. In the current study, defined epithelial structures were difficult to form once the culture time was extended to 3 weeks. A similar phenomenon has also been reported in 3D gel systems.[23] This result is likely due to (1) imbalanced growth rate between MCF10A cells and preadipocytes due to the faster proliferation of MCF10A cells and (2) limited mass transport caused by the increased ECM density secreted by cocultured cells. Thus, to further optimize this 3D coculture model *in vitro*, alternative mammary epithelial cell lines may be useful and bioreactor perfusion would be useful to explore in future studies.

In conclusion, we have characterized a novel 3D coculture model to study mammary epithelial–stromal interactions under defined and physiologically relevant conditions. It is hoped that utilization of this epithelial–preadipocyte model system with cells from unmodified and genetically engineered knockout or transgenic hosts will allow the identification and characterization of the factors that control the developmental fate of normal and tumorigenic cells in the mammary gland. Further, this information should lead to

the development of novel therapies to effectively prevent and/or treat breast cancer.

Acknowledgments

We appreciate the significant technical contributions by Carmen Preda. This work was supported by Phillip Morris International (CS) and the NIH P41 Tissue Engineering Resource Center (P41 EB002520) (DK).

Disclosure Statement

No competing financial interests exist.

References

1. Cunha, G.R., Young, P., Christov, K., Guzman, R., Nandi, S., Talamantes, F., and Thordarson, G. Mammary phenotypic expression induced in epidermal cells by embryonic mammary mesenchyme. Acta Anat **152,** 195, 1995.
2. Barcellos-Hoff, M.H., and Ravani, S.A. Irradiated mammary gland stroma promotes the expression of tumorigenic potential by unirradiated epithelial cells. Cancer Res **60,** 1254, 2000.
3. Maffini, M.V., Soto, A.M., Calabro, J.M., Ucci, A.A., and Sonnenschein, C. The stroma as a crucial target in rat mammary gland carcinogenesis. J Cell Sci **117,** 1495, 2004.
4. Wozniak, M.A., and Keely, P.J. Use of three-dimensional collagen gels to study mechanotransuction in T47D breast epithelial cells. Biol Proced Online **7,** 144, 2005.
5. Barcellos-Hoff, M.H., Aggeler, J., Ram, T.G., and Bissell, M.J. Functional differentiation and alveolar morphogenesis of primary mammary cultures on reconstituted basement membrane. Development **105,** 223, 1989.
6. Roskelley, C.D., Desprez, P.Y., and Bissell, M.J. Extracellular matrix-dependent tissue-specific gene expression in mammary epithelial cells requires both physical and biochemical signal transduction. Proc Natl Acad Sci USA **91,** 12378, 1994.
7. Zangani, D., Darcy, K.M., Shoemaker, S., and Ip, M.M. Adipocyte-epithelial interactions regulate the *in vitro* development of normal mammary epithelial cells. Exp Cell Res **247,** 399, 1999.
8. Weins, D., Park, C.S., and Stockdale, F.E. Milk protein expression and ductal morphogenesis in the mammary gland *in vitro*: hormone-dependent and -independent phases of adipocyte-mammary epithelial cell interaction. Dev Biol **120,** 245, 1987.
9. Beck, J.C., and Hosick, H.L. Growth of mouse mammary epithelium in response to serum-free media conditioned by mammary adipose tissue. Cell Biol Int Rep **12,** 85, 1988.
10. Huss, F.R., and Kratz, G. Mammary epithelial cell and adipocyte co-culture in a 3D matrix: the first step towards tissue-engineered human breast tissue. Cells Tissues Organs **169,** 361, 2001.
11. Debnath, J., Muthuswamy, S.K., and Brugge, J.S. Morphogenesis and oncogenesis of MCF-10A mammary epithelial acini grown in three-dimensional basement membrane cultures. Methods **30,** 256, 2003.
12. Schedin, P., Mitrenga, T., McDaniel, S., and Kaeck, M. Mammary ECM composition and function are altered by reproductive state. Mol Carcinog **41,** 207, 2004.
13. Wang, Y., Kim, H.J., Vunjak-Novakovic, G., and Kaplan, D.L. Stem cell-based tissue engineering with silk biomaterials. Biomaterials **27,** 6064, 2006.
14. Hofmann, S., Knecht, S., Langer, R., Kaplan, D.L., Vunjak-Novakovic, G., Merkle, H.P., and Meinel, L. Cartilage-like tissue engineering using silk scaffolds and mesenchymal stem cells. Tissue Eng **12,** 272, 2006.
15. Mauney, J.R., Nguyen, T., Gillen, K., Kirker-Head, C., Gimble, J.M., and Kaplan, D.L. Engineering adipose-like tissue *in vitro* and *in vivo* utilizing human bone marrow and adipose-derived mesenchymal stem cells with silk fibroin 3D scaffolds. Biomaterials **28,** 5280, 2007.
16. Soffer, L., Wang, X., Zhang, X., Kluge, J., Dorfmann, L., Kaplan, D.L., and Leisk, G. Silk-based electrospun tubular scaffolds for tissue-engineered vascular grafts. J Biomater Sci Polym Ed **19,** 653, 2008.
17. Wang, Y., Kim, U.J., Blasioli, D.J., Kim, H.J., and Kaplan, D.L. *In vitro* cartilage tissue engineering with 3D porous aqueous-derived silk scaffolds and mesenchymal stem cells. Biomaterials **26,** 7082, 2005.
18. Dubois, S.G., Floyd, E.Z., Zvonic, S., Kilroy, G., Wu, X., Carling, S., Halvorsen, Y.D., Ravussin, E., and Gimble, J.M. Isolation of human adipose-derived stem cells from biopsies and liposuction specimens. Methods Mol Biol **449,** 69, 2008.
19. Wang, X., Wang, W., Ma, J., Guo, X., and Ma, X. Proliferation and differentiation of mouse embryonic stem cells in APA microcapsule: a model for studying the interaction between stem cells and their niche. Biotechnol Prog **22,** 791, 2006.
20. Soriano, J.V., Pepper, M.S., Nakamura, T., Orci, L., and Montesano, R. Hepatocyte growth factor stimulates extensive development of branching duct-like structures by cloned mammary gland epithelial cells. J Cell Sci **108,** 413, 1995.
21. Kilroy, G.E., Foster, S.J., Wu, X., Ruiz, J., Sherwood, S., Heifetz, A., Ludlow, J.W., Stricker, D.M., Potiny, S., Green, P., Halvorsen, W.C., Cheatham, B., Storms, R.W., and Gimble, J.M. Cytokine profile of human adipose-derived stem cells: expression of angiogenic, hematopoietic, and pro-inflammatory factors. J Cell Physiol **212,** 702, 2007.
22. Darcy, K.M., Zangani, D., Shea-Eaton, W., Shoemaker, S.F., Lee, P.P., Mead, L.H., Mudipalli, A., Megan, R., and Ip, M.M. Mammary fibroblasts stimulate growth, alveolar morphogenesis, and functional differentiation of normal rat mammary epithelial cells. In Vitro Cell Dev Biol Anim **36,** 578, 2000.
23. Krause, S., Maffini, M.V., Soto, A.M., and Sonnenschein, C. A novel 3D *in vitro* culture model to study stromal-epithelial interactions in the mammary gland. Tissue Eng Part C Methods **14,** 261, 2008.
24. Sadlonova, A., Novak, Z., Johnson, M.R., Bowe, D.B., Gault, S.R., Page, G.P., Thottassery, J.V., Welch, D.R., and Frost, A.R. Breast fibroblasts modulate epithelial cell proliferation in three-dimensional *in vitro* co-culture. Breast Cancer Res **7,** R46, 2005.
25. Weaver, V.M., Howlett, A.R., Langton-Webster, B., Petersen, O.W., and Bissell, M.J. The development of a functionally relevant cell culture model of progressive human breast cancer. Semin Cancer Biol **6,** 175, 1995.
26. Tajima, H., Higuchi, O., Mizuno, K., and Nakamura, T. Tissue distribution of hepatocyte growth factor receptor and it's exclusive down-regulation in a regenerating organ after injury. J Biochem **111,** 401, 1992.
27. Beviglia, L., Matsumoto, K., Lin, C.S., Ziober, B.L., and Kramer, R.H. Expression of the c-Met/HGF receptor in human breast carcinoma: correlation with tumor progression. Int J Cancer **74,** 301, 1997.
28. Nelson, C.M., and Bissell, M.J. Modeling dynamic reciprocity: engineering three-dimensional culture models of breast

architecture, function, and neoplastic transformation. Semin Cancer Biol **15,** 342, 2005.
29. Gudjonsson, T., Rønnov-Jessen, L., Villadsen, R., Rank, F., Bissell, M.J., and Petersen, O.W. Normal and tumor-derived myoepithelial cells differ in their ability to interact with luminal breast epithelial cells for polarity and basement membrane deposition. J Cell Sci **115,** 39, 2002.
30. Karagiannides, I., Tchkonia, T., Dobson, D.E., Steppan, C.M., Cummins, P., Chan, G., Salvatori, K., Hadzopoulou-Cladaras, M., and Kirkland, J.L. Altered expression of C/EBP family members results in decreased adipogenesis with aging. Am J Physiol Regul Integr Comp Physiol **280,** 6, 2001.

Address correspondence to:
David L. Kaplan, Ph.D.
Departments of Biomedical and Chemical and Biological Engineering
Tufts University
4 Colby St.
Medford, MA 02155

E-mail: david.kaplan@tufts.edu

Received: December 11, 2008
Accepted: April 1, 2009
Online Publication Date: July 16, 2009